

Fast Ignition Studies at Sandia National Laboratories

R. B. Campbell, M. E. Cuneo, D. L. Hanson, M.K. Matzen, T. A. Mehlhorn, J. L. Porter, S.A. Slutz, and R.A. Vesey.

Sandia National Laboratories, Albuquerque, New Mexico 87185, USA

Abstract. This talk will describe ongoing and planned fast ignition theoretical and experimental work using the Z-machine in concert with the upgraded Z-Beamlet/PW laser system. Z can produce x-ray powers of 100-250TW, x-ray energies 1-1.8MJ, and $> 200\text{eV}$ radiation temperatures and thus represents an interesting platform for compressing large quantities of matter for use as fast ignition targets. Soon Z will undergo refurbishment, and the resulting parameters for Z-R are even more interesting. The Z-Beamlet system is currently undergoing short pulse conversion with the plan that Z-Beamlet/PW will deliver 0.5-2 kJ in 0.5-10 psec in FY07 when Z-R will be available. Numerical simulations of laser/plasma interaction, electron transport, and ion generation at relevant densities are being performed using LSP, a 3D implicit hybrid PIC code. LASNEX simulations of the compression of deuterium/tritium fuel in various reentrant cone geometries are being performed. Analytic and numerical modeling has been performed to determine the conditions required for fast ignition breakeven scaling. These theoretical results indicate that to achieve fusion output equal to the energy deposited by fast particles will require about 5% of the laser energy needed for ignition and might be an achievable goal (within a factor of 2) with Z-Beamlet/PW.

Keywords: Fast Ignition, Fusion, Z-Pinch, Z-Beamlet, GEKKO/PW/

PACS: 52.57.Kk, 52.65Rr

I. THE Z ACCELERATOR AND Z PINCH LOADS

The z pinch was one of the earliest techniques used as an attempt to heat plasmas to thermonuclear temperatures[1]. Sandia National Laboratories began a program in the 1970s on the Proto II [2] pulsed power generator to study the efficacy of using x rays from pulsed-power-driven z-pinch implosions to compress a DT-filled spherical capsule. In a z pinch, the azimuthal magnetic field associated with the axial flow of current through a cylindrically symmetric plasma creates a magnetic pressure from the $J \times B$ or Lorentz force that accelerates the plasma radially inward at high velocities. X rays are produced when the imploding plasma stagnates on the cylindrical axis of symmetry. A breakthrough in the x-ray power was achieved in 1995 when a series of experiments[3] performed on the 7 MA, 20 TW electrical Saturn[4] pulsed power generator revealed that the x-ray power from an imploding z pinch could be greatly enhanced by using a cylindrical array containing a very large number of wires (>100). This breakthrough technology was quickly adapted for testing at higher currents. The Particle Beam Fusion Accelerator (PBFA II) [5] was modified to allow z-pinch

experiments at 20MA (PBFA-Z) and was completed in October 1996. The facility is now called Z [6].

The Z facility is shown in Figure 1a. Z delivers 11.5 MJ stored energy, 19 MA peak load current, 40 TW electrical power to load resulting in 100-250 TW x-ray power at 1-1.8 MJ x-ray energy. There is a plan starting in 2006 to ‘refurbish’ Z, the resulting facility referred to as ‘ZR’. The refurbished components should be installed that year and, after a testing phase, Z will return to full operational status in 2007. For typical z-pinch configurations, the delivered current should increase more than 30%, which corresponds to an energy increase of 70%, thereby allowing access to a new high energy density physics regime. A liquid cryogenic D₂ hemispherical capsule[7] is being developed (see section II) with a thin inner shell to contain the D₂ layer, based on the system previously developed[8] for cryogenic D₂ EOS measurements on Z.[9] Radiation symmetry control in this system may be sufficient in the fast ignition application to produce densities of 135 g/cm³ for a compressed fuel ρr of 0.8–1.1 g/cm² with hemispherical implosions on Z-R[10]. A concept called a dynamic hohlraum [11] (Figure 1b2) can produce higher radiation temperatures than vacuum hohlraum drive (Figure 1b1) and may produce average densities of up to 300 g/cm³ (a ρr of 1.3 g/cm² at 180 eV).

The multi-kilojoule, multi-terawatt (0.3–20 ns) Z-Beamlet Laser[12] (ZBL), originally a scientific prototype at Lawrence Livermore National Laboratory for the laser system of the National Ignition Facility[13] (NIF), was completed and implemented at Z. This system is currently undergoing a short pulse upgrade which will enable it to deliver 0.5-2 kJ in 0.5-10 psec in FY07 when ZR will be online. The development of this high-energy (2 kJ), short-pulse (petawatt) laser coupled to the ZR should allow exploration, on the 2008 time frame, of fast ignition science issues such as the production of high-energy electron and ion beams, beam-matter coupling at high densities and temperatures, and fuel heating and sub-ignition fusion neutron yields.[10,14].

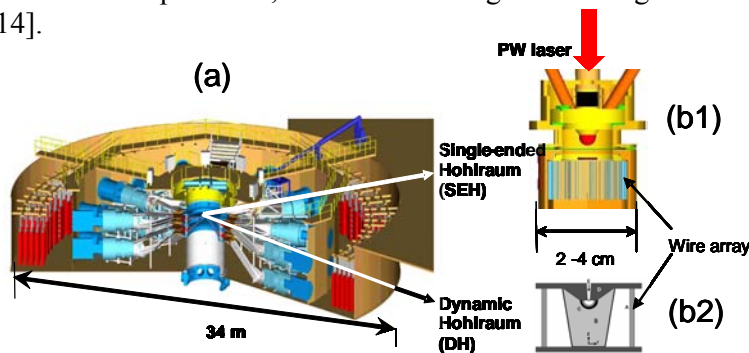


FIGURE 1. The Z accelerator (a) and two typical loads for fast ignition. (b1) is the single ended hohlraum, and (b2) is the dynamic hohlraum.

Figure 1b shows two different fast ignition loads: Figure 1b1 shows a hemispherical capsule located in a secondary hohlraum which is driven by X-rays generated by a single wire array in the primary hohlraum. This load is called a single ended hohlraum (SEH), and Figure 1b2 shows the more efficient dynamic hohlraum (DH) [15] which integrates the hemisphere and wire array more intimately. The hemisphere is

encapsulated in shaped foam; the hohlraum radiation case is the wire array itself. The DH, by virtue of its smaller volume, will create higher radiation temperature at the expense of reduced symmetry. Once compressed, the Z-Beamlet/PW laser heats the compressed core. Fast ignition reduces the symmetry and convergence ratio requirements for the capsule implosion. Z's X-ray generation capabilities makes it effective through indirect drive in compressing significant quantities of matter to a highly compressed state, particularly using the DH. Experiments would likely be performed first in the SEH configuration which separates the wire array and capsule implosion physics because it would afford easier diagnostic access and more developed simulation capability. Later experiments would then capitalize on the higher temperatures associated with the DH.

II. HEMISPHERICAL FAST IGNITION TARGETS

Implosion of hemispherical shells in contact with a high density glide plane has been studied [16]. This fast ignitor fuel assembly configuration well adapted to a SEH or DH z-pinch indirect radiation drive.. This hemispherical fast ignitor geometry is a special case of the “cone-in-shell” geometry for spherical capsules, with the reentrant cone opened to 180° to form a planar glide surface for the imploding hemisphere. Such a shell is shown in Figure 2.



FIGURE 2. Open target mount with hemispherical capsule on 30- μm -thick gold disc.

In experiments on the Z accelerator (20 MA peak current), hemispherical GDP (glow discharge polymerization) capsule implosions in cylindrical secondary hohlraums were heated to 90-100 eV by a single 120 TW wire-array zpinch. The implosions were imaged using both point-projection backlighting[12] and crystal imaging radiography techniques [17]. Below (Figure 3) is shown a typical image from point projection radiography.

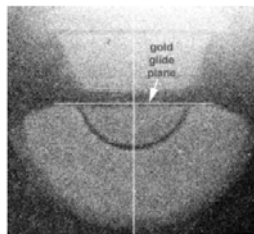


FIGURE 3. Point projection radiograph of hemi-capsule implosion for shot Z1045 at 6.0 ns beyond time of peak pinch radiation.

For indirect drive, the observation of complex hydrodynamic motion at the capsule/plane interface is complicated by plasma expansion from the glide plane. Simulations of capsule implosions show reasonable agreement with experiment at a convergence of 2. Figure 4 shows a comparison of radiographs obtained experimentally using a 6.7 keV backlighter with Lasnex simulations of the implosion for a convergence ratio of 2.

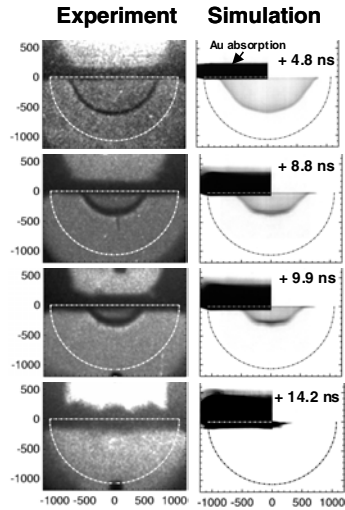


FIGURE 4. Real (left) and synthetic (right) backlighter images of the implosion of GDP capsules on a gold glide plane.

Below is a more quantitative comparison table of the normalized Legendre coefficients for the experiments and Lasnex simulations for orders 2,4,6,8, showing reasonable agreement.

TABLE 1 Comparison of Simulation and Experiment for Shot Z923 - Hemispherical Capsule Implosion in Pole-Hot Secondary Geometry.

8th-order Legendre fit to limb shape:		
Mode	Experiment	Simulation
a_2/a_0	-14.7%	-11.8%
a_4/a_0	+5.0%	+3.5%
a_6/a_0	-1.7%	-2.4%
a_8/a_0	-0.2%	+1.3%
where: $a_0 = 520 \mu\text{m}$		

The OPTSEC viewfactor code [18] simulations shown in this table predicts dominant P2 and P4 modes with correct signs to produce the experimentally observed limb shape for the pole-hot secondary flux geometry. The P2 and P4 modes from the synthetic backlit image with OPTSEC calculated asymmetry are somewhat smaller than those from the experiment. A more pole-hot drive with somewhat higher levels of

P2 and P4 would result from a simulation using an imploding pinch x-ray source, rather than the static on-axis pinch assumed in the present OPTSEC calculations.

More recently, experiments have been performed where images were obtained of hemispherical implosions at a convergence ratio of 10.[19]. Corresponding simulations like those found in Figure 4 have not been performed so far in this case.

Below (Figure 5) is a conceptual design for a DT-filled double shell hemisphere for use in an advanced fast ignition target [16]. The hemisphere is not only a good match to the asymmetric x-ray implosion drive, but offers distinct topological advantages for liquid cryogenic fuel delivery systems over the gold cone configuration. Initial target fabrication studies are presently being conducted at Sandia.

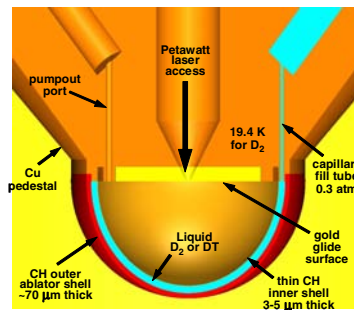


FIGURE 5. Conceptual design for a DT-filled double shell hemisphere for use in an advanced ignition target.

III. TARGET COMPRESSION AND PULSE SHAPING

For central hot-spot ignition, it is the spherical convergence of a series of precisely timed shocks which determines whether the capsule ignites and this therefore places strict requirements on the radiation pulse shape that creates the shocks. In fast ignition, the short-pulse laser-produced particles provide the igniting spark to the fuel. A variety of radiation pulse shapes that may not provide a self-ignited hot spot will typically still produce high fuel density and ρr ; hence the relaxed pulse-shaping requirements for fast ignition. However, pulse-shaping is still important in fuel assembly as a means to obtain high fuel density for a given driver energy. One simple approach to “passive” pulse-shaping for the single-sided hohlraum uses a burnthrough filter at the entrance to the secondary hohlraum[10], as shown in figure 6. The proper choice of filter material and thickness allows the pinch run-in radiation to be absorbed, burning through during the rising main power pulse to produce a simple foot and main peak structure in the resulting capsule drive pulse.

A variety of techniques to actively produce shaped radiation pulses from z-pinch implosions have been envisioned, and some have been experimentally tested. These include work on nested wire arrays and wire arrays imploding onto x-ray converter targets[20]. Many of the experiments cited were aimed at improving the quality of the z-pinch implosion (i.e. increasing the peak x-ray power), or at characterizing the dynamic hohlraum created inside the imploding z-pinch, but they also demonstrate pulse-shaping techniques that may prove useful for driving capsule implosions in vacuum hohlraums. With the many combinations of current transfer nested wire

arrays, collisional x-ray converters, and burnthrough filter transmission available, the potential for z-pinch vacuum hohlraums to provide pulse shapes suitable for dense fuel assembly appears promising and will be explored in future simulations and experiments.

Using a passive pulse-shaping technique, beta-layered cryogenic DT ice-fueled hemispherical capsules have been designed for such a system. Initial one-dimensional scoping calculations using Lasnex [21] predicted peak densities of 150 g/cm^3 and peak fuel pd of 0.6 g/cm^2 were feasible using the pulse shape shown in Figure 6.

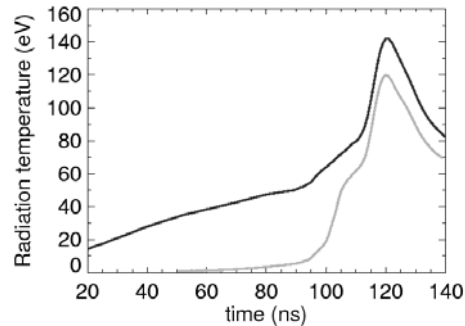


FIGURE 6. Radiation temperature shape for the primary (black) and secondary (grey) hohlraum regions in a SEH, using passive pulse shaping techniques.

The capsules have an outer radius of 1.05 mm, consisting of a $80 \mu\text{m}$ thick DT fuel layer surrounded by a $50 \mu\text{m}$ thick plastic (CH) ablator. These 1D simulations were followed up with two-dimensional simulations focusing on the capsule and glide surface material, of the type now described.

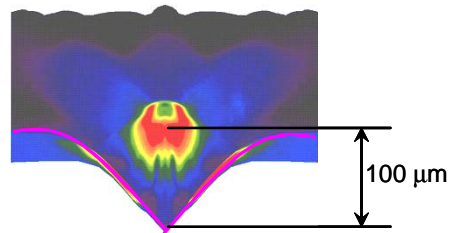


FIGURE 7. Compressed hemispherical shell driven by the secondary hohlraum radiation pulse of Figure 6. The gold glideplane is outlined in magenta. The PW laser is directed vertically upward through the ‘tip’ of the distended glideplane.

Figure 7 shows an example of an assembled fuel configuration at the time of peak fuel density. By changing the secondary hohlraum geometry (length, shine shield radius), the pole-hot nature of the x-ray flux incident on the capsule may be tuned. In particular, a larger separation of the capsule from the primary hohlraum results in a more pole-hot flux distribution, a characteristic of the illustrated profile. For the hemispherical capsule shown and a $50\text{-}\mu\text{m}$ thick gold glide plane, the case shown has an 20% time-integrated P2, and a 35% pole/equator asymmetry which gives a centrally peaked imploded configuration. This case also results in considerable distortion and breakthrough of the gold due to the capsule stagnation shock. Note also that hot laser generated particles must traverse a halo plasma on the order of $100 \mu\text{m}$.

This case, which gave a DT fuel density peaking at 90 g/cm^3 and on-axis $\rho\Delta z$ of 0.8 g/cm^2 , has been used as the starting point for electron transport and heating simulations using the LSP code. Examples of assembled mass heating as it pertains to the Osaka GEKKO/PW experiments and ZR are discussed in the next section.

IV. HEATING OF ASSEMBLED MASS

Recently, state-of-the-art simulations of the coupling of a short-pulse, high-intensity laser pulse to matter[22] with the LSP code[23] have been used to model the fast ignition experiments of Kodama et al.[24].

LSP (Large Scale Plasma) code is a 3-D implicit hybrid PIC code. In these simulations, LSP was run in a 2-D, cylindrically symmetric, implicit hybrid mode. In light of the implicit energy conserving algorithms for the hybrid species, the spatial cell size is permitted large compared to both the skin depth and Debye length. This enables us to perform parametric studies of geometries on the order of $100 \text{ }\mu\text{m}$ at densities of a few times 10^{25} cm^{-3} on current supercomputers. The price paid is the loss of spatial and temporal resolution at the smallest scales, on the order of the skin depth and the electron plasma period. The important collective electromagnetic (EM) effects (e.g. return current, large-scale filamentation) are included self-consistently, although skin depth scale collisionless Weibel-type filamentation in very low-density regions ($<10^{22} \text{ cm}^{-3}$) is not resolved, for reasons of practical resolution limits for these integrated simulations. The 2D treatment give a reasonable approximation to reality as far as effects we want to show, but the real details of hosing and small scale filament structure have, of course, a three dimensional character. Such 3-D simulations are in progress, including the full laser/plasma interaction and will be the subject of a future publication.

The initial conditions in the simulation for the background mass density are assumed from a combination of a 2D hydrodynamic calculation and shadowgraphy measurements of the compressed core on GEKKO-PW as shown in Ref. [25]. An axial slice of background electron density used in the simulation is shown in Fig. 8.

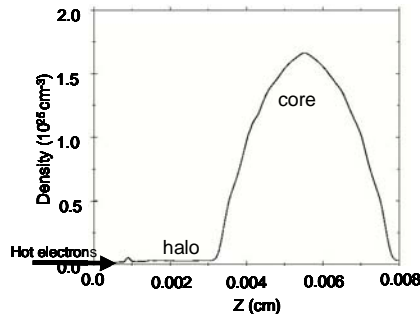


FIGURE 8. Axial slice of electron density of halo and core for the simulations of the GEKKO/PW data. Hot electrons are injected from the left in the positive Z direction.

The four PIC fluid species included in the simulations are “cold” electrons, D^+ ; C^{+3} (deuterated plastic (CD) shell), and Au^{+25} (cone remnant). The kinetic species are the kinetic laser-generated hot electrons and kinetic hot electrons “promoted” from the fluid electrons when their ratio of directed velocity to spread exceeds a threshold.

The background temperature is initially uniform at 300 eV, the value in accordance with experimental measurements; although a uniform spatial distribution was assumed for simplicity. The laser-produced electrons are assumed to be distributed in a relativistic Maxwellian with a temperature along the injection direction of 1.4 MeV, and an angular spread of 22.5° , both consistent with experimental estimates. We estimate the generation efficiency of laser energy to hot electron energy to be 33%, yielding 100 J of electrons injected. The current time history mimics the experimental laser intensity profile that is a Gaussian pulse, with a full width of 600 fsec. The current density radial distribution is assumed Gaussian with a $30\mu\text{m}$ full width with a peak current of 119 MA.

We now compare the simulation results with the ion temperature data taken from the PW experiments. The ion temperature was measured with a neutron time-of flight detector, showing a deuterium temperature of 0.8 ± 0.1 keV. Figure 9 shows the linear contours of deuterium temperature simulated by LSP for the GEKKO-PW

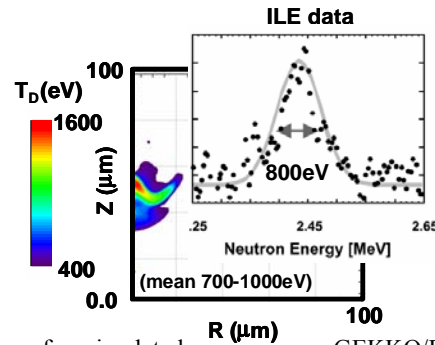


FIGURE 9. Contours of simulated GEKKO/PW core temperature deuterium (linear) in eV for the illustrative case at 4.3 psec. Data is also shown for comparison.

parameters. Note that the shape of the heated region is not spherical, but instead characteristic of localized heating on the near side of the density gradient. The highest temperature in the simulation is on the order of 1.5 keV on the near side of the core, but a much larger volume at high-density is at a temperature from 0.8–1.1 keV, in reasonable qualitative agreement with the data shown. The DD fusion reaction weighted ion temperature is the most germane for comparison with a single measurement and is about 0.9-1 keV from the simulation.

The apparent physical mechanism for the anomalous stopping will now be considered. The fluctuating magnetic field creates an electric field directed to slow down the hot electrons so that the effective range is reduced to less than or equal to the core ρL . In the stopping process, the fluctuating magnetic fields cause the background electrons to execute chaotic orbits that appear macroscopically as an additional plasma resistivity. The higher resistivity drives a correspondingly larger electric field to maintain the return current, and this field, in turn, slows down the hot electrons.

A central issue for fast ignition is the efficiency by which the laser light is converted to core thermal energy. There are several factors that reduce the efficiency of energy deposition in the compressed core. First, there is parasitic heating in the halo plasma due to the establishment of the return current necessary to adhere to the Alfvén current limit [26], which accounts for about 10% losses in GEKKO/PW. This loss may

be more for envisioned higher intensity lasers that drive higher currents in ignition-class systems. The largest loss is attributable to hot particles streaming around the core, and accounts for 57% of the losses of hot particle in the Osaka experiments. While there is some evidence of magnetic channeling of the electrons, the spread in the laser-produced electron distribution is enough to cause this level of losses. The remaining 33% of the electron energy is deposited in the compressed core. Combined with the 33% laser to electron conversion efficiency, the simulations suggest that slightly less than 10% of the laser energy ends up in the core as thermal energy of the compressed core.

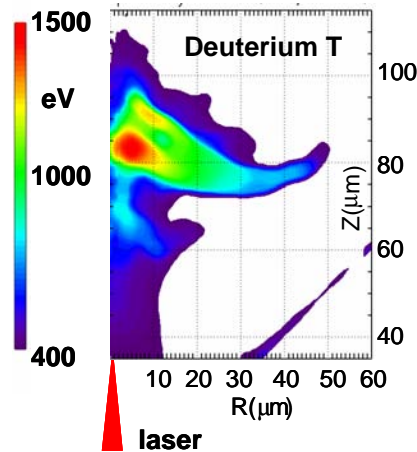


FIGURE 10. A heating simulation at 2kJ laser energy of a hemi-shell compressed with ZR X-rays. The peak temperature of approximately 1.5 keV occurs below the peak density at about 40 g/cm^3 ,

Having compared favorably the code results with the Osaka data, cores at somewhat higher density using the same physics assumptions are now considered. These cores are formed by the compression of a hemispherical shell by a single ended hohlraum driven by X-rays produced by ZR. The mass density profile is shown in Figure 7. Figure 10 shows the result of an LSP simulation of the injection of 0.6 kJ (33% laser to electron conversion efficiency) of electrons in a Maxwellian distribution with a 1.4MeV energy (scaled from GEKKO) and 22.5° angular spread. The peak temperature exceeds 1.5keV at a DT density of 40 g/cm^3 . While the assembled mass ρr is about 0.8 g/cm^2 , the mass heated above 1keV is more germane for neutron yield and energy output, and is about 0.1 g/cm^2 .

The simulations of the GEKKO/PW data with LSP and predictions for Z Beamlet/PW-ZR seem encouraging, however not all the physics has been incorporated yet. Most notably absent is the self-consistent generation of the hot electrons through the laser/plasma interaction process. Work is progressing toward this goal, but it is particularly difficult treat the transition from the critical density layer laser physics on the front side through the halo to the very high density core, and preserve good energy conservation.

It should be mentioned in passing that LSP is also quite useful in understanding other PW laser-related problems. It is currently being used to design targets for K_α

backlighting, proton radiography and deflectometry, and to study the anomalous stopping of hot electrons in matter.

V. BREAKEVEN SCALING

FI ignition scaling was studied at length by Atzeni [27]. In this work, the hot particle energy, intensity, pulse length, and power to ignite the pre-compressed core was studied as a function of hot particle penetration and core density. Recently [28], a similar methodology was employed to look at scaling of systems at deposited energy breakeven. This is defined as the fusion energy output divided by the energy deposited in the core equal to unity; $Q=1$. For cores that are tamped by surrounding cold material, the energy for breakeven scales as $E(\text{kJ})=7.5(\rho/100)^{-1.87}$ about a factor of 20 smaller than the corresponding ignition energy. The strong dependence on density favors the higher densities obtainable with the dynamic hohlraum described in Section I. For the lower breakeven energy to apply, the cores must not only be denser, but correspondingly smaller. This may make it more difficult to deposit energy in the core in light of the relatively large fraction of the hot electrons that miss the core (57%) for a relatively large core (50 μm) in GEKKO/PW simulations. To illustrate the dependence of Q on deposited energy and density/core size, contour plots like the one shown in Figure 11 below:

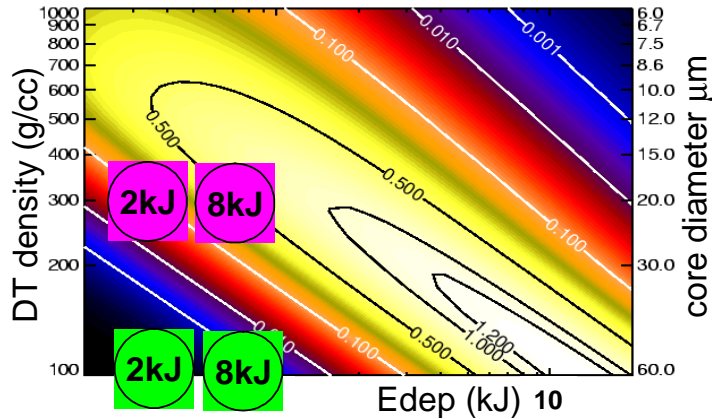


FIGURE 11. Contours of the deposited energy breakeven parameter, Q . These simulations were performed at a ρd of 0.6 g/cm^2 and a pulse length of 5psec. The green circles are LSP/Lasnex simulations with a SEH on ZR, the magenta circles are estimates of performance with the DH with ZR performance.

The $Q=1$ surface at minimum deposited energy is at about $E_{\text{dep}}=1.7\text{kJ}$, for $\rho=300 \text{ g/cm}^3$, and a core diameter of $20\mu\text{m}$. To attain $Q=0.1$ at $\rho=300 \text{ g/cm}^3$ requires about 200J of deposited energy. The corresponding $Q=0.5$ surface at requires 800J of deposited energy. The dynamic hohlraum concept can deliver high temperatures; over 200eV has been demonstrated experimentally [11]. Simulations with proper radiation pulse shaping have suggested ρ average of 300g/cm^3 at a temperature of 180 eV [29].

For backlighting, Z-Beamlet/PW is rated conservatively as a 0.5-2kJ system. The current facility only supports one large aperture laser, and populating the other 3

potential beamlines is not envisioned at this time. With this one line system, the 500J level uses gold gratings, and 2kJ requires advanced multi-layer dielectric (MLD) gratings still under development worldwide, and beam expansion through the amplifiers. The short pulse system operating at 2kJ could deposit 200J into the core, possibly reaching $Q=0.1$. However, if it was deemed interesting, the laser energy for 4 beamlines could, in principle, be increased to about 8kJ. If the 10% laser to deposited electron in core efficiency is applied as computed for GEKKO/PW, we could expect 800J to be deposited. From Figure 10, that energy would put the system on the $Q=0.5$ curve at a density which is at least theoretically achievable with the DH and ZR.

VI. CONCLUSIONS

In this paper, the effort at Sandia National Laboratories in the fast ignition arena has been reviewed. Owing to Z and ZR's significant X-ray output, it could be an interesting facility for compressing large quantities of matter, particularly utilizing the dynamic hohlraum (DH). A target design effort is underway under which hemispheres have been compressed to a convergence ratio of up to 10 with Z. Double shell targets for cryogenic fuel compression are currently being fabricated. Simulations suggest that pulse shapes can be designed via various schemes to compress matter with single ended or dynamic hohlraum loads to the requisite densities (300 g/cm^3) and sizes ($20 \mu\text{m}$) to make them energetically interesting for fast ignition science studies. A refurbished Z (ZR) and short pulse upgrade to Z-Beamlet will be available in the 2007 timeframe that will deliver nominally 0.5-2kJ, and could potentially be upgraded (with multiple beamlines, advanced components and technologies) to 6-8kJ. Implicit PIC simulations of core heating by laser-produced electrons using the LSP code have been compared favorably with GEKKO/PW experiments, and are being used to design FI heating experiments for ZR. Using laser to core thermal energy efficiencies of around 10% computed with LSP, and energy breakeven scaling derived semi-analytically, Q values of 7-10% for 2kJ, 20-30% for the 6kJ system, and $Q=50\%$ for the 8kJ case all appear possible for a dynamic hohlraum load with average core densities of 300 g/cm^3 . These advances so far seem quite encouraging for the development of fast ignition on the Z platform.

The primary use of Z-Beamlet/PW will be high energy backlighting. Backlighting with Z-Beamlet has played a crucial role in the understanding of wire array physics and capsule symmetry. The short pulse upgrade will improve this diagnostic since it will now be able to penetrate denser objects attainable with the higher X-ray energy of ZR. Demonstration of short pulse laser/ZR accelerator coupling for backlighting and progress on fast ignition science issues, (e.g. electron and ion production, target coupling and heating efficiency) beginning on the 2008 timeframe would be required prior to future Z Beamlet/PW upgrades. Nevertheless, the results presented here suggest the potential to reach nearly deposited energy breakeven for fast ignition, which is an important milestone on the path to ignited ICF plasma.

VII. ACKNOWLEDGMENTS

We wish to thank R. Kodama for the use of the ILE data used in Figure 9. Sandia is a multiprogram laboratory operated by Sandia Corporation, a Lockheed Martin Company, for the United States Department of Energy's National Nuclear Security Administration under contract DE-AC04-94AL85000.

VIII. REFERENCES

1. A. S. Bishop, *Project Sherwood: The U.S. Program in Controlled Fusion*, U.S. Atomic Energy Commission (Addison-Wesley, Reading, MA, 1958).
2. T. H. Martin, J. P. VanDevender, D. L. Johnson, D. H. McDaniel, and M. Aker, *Proceedings of the International Topical Conference on Electron Beam Research and Technology, Albuquerque, NM, 1976*, edited by G. Yonas (Sandia Laboratories, New Mexico, 1977), Vol. 1, p. 450. See National Technical Information Service Document No. SAND76-5122. Copies may be ordered from the NTIS, Springfield, VA 22161.
3. T. W. L. Sanford, G. O. Allshouse, B. M. Marder, T. J. Nash, R. C. Mock, R. B. Spielman, J. F. Seamen, J. S. McGurn, D. O. Jobe, T. L. Gilliland *et al.*, *Phys. Rev. Lett.* **77**, 5063 (1996).
4. D. D. Bloomquist, R. W. Stinnett, D. H. McDaniel, J. R. Lee, A. W. Sharpe, J. A. Halbleib, L. G. Schlitt, P. W. Spence, P. Corcoran, *Proceedings of the Sixth International Pulsed Power Conference, Arlington, VA, 1987*, edited by P. J. Turchi and B. H. Bernstein (IEEE, New York, 1987), Vol. 1, p. 310.
5. B. N. Turman, T. H. Martin, E. L. Neau *et al.*, *Proceedings of the Fifth International Pulsed Power Conference, Arlington, VA, 1985*, edited by M. F. Rose and P. J. Turchi (IEEE, New York, 1985), Vol. 1, p. 155.
6. R. B. Spielman, W. A. Stygar, J. F. Seamen *et al.*, *Proceedings of the 11th International Pulsed Power Conference, Baltimore, MD, 1997*, edited by G. Cooperstein and I. Vitkovitsky (IEEE, Piscataway, NJ, 1997), Vol. 1, p. 709.
7. D. L. Hanson, S. A. Slutz, R. A. Vesey, and M. E. Cuneo, to be published *Fusion Sci. Technol.* (2006).
8. D. L. Hanson, R. R. Johnston, M. D. Knudson, J. R. Asay, C. A. Hall, J. E. Bailey, and R. J. Hickman, in *Shock Compression of Condensed Matter-2001*, edited by M. D. Furnish, N. N. Thadhani, and Y. Horie (AIP, Melville, NY, 2002), p. 1
9. M. D. Knudson, D. L. Hanson, J. E. Bailey, C. A. Hall, J. R. Asay, and W. W. Anderson, *Phys. Rev. Lett.* **87**, 225501 (2001).
10. R.A. Vesey, *et. al.* to be published *Fusion Science and Technology* (2006).
11. S. A. Slutz, J. E. Bailey, G. A. Chandler *et al.*, *Phys. Plasmas* **10**, 1875 (2003).
12. P.K. Rambo, I.C. Smith, J.L. Porter, *et.al.* *Appl. Optics*, **44**, 2421 (2005) see also G. R. Bennett, O. L. Landen, R. F. Adams, J. L. Porter, L. E. Ruggles, W. W. Simpson, and C. Wakefield, *Rev. Sci. Instrum.* **72**, 657 (2001).
13. J. A. Paisner, E. M. Campbell, and W. J. Hogan, *Fusion Technol.* **26**, 755, (1994).
14. S. A. Slutz, R. A. Vesey, I. Shoemaker, T. A. Mehlhorn, and K. Cochrane, *Phys. Plasmas* **11**, 3483 (2004).
15. S.A. Slutz, J.E. Bailey, G.A. Chandler, *et. al.* *Phys. Plasmas*, **10**, 1875 (2003).
16. D.L. Hanson, R.A. Vesey, D.B. Sinars, M.E. Cuneo, S.A. Slutz, J.L. Porter. *Third International Conference on Inertial Fusion Sciences and Applications (IFSA 2003)*, 7-12 Sept. 2003, Monterey, CA, USA; p.359-63
17. D.B. Sinars, G.R. Bennett, D.F. Wenger, M.E. Cuneo, J.L. Porter. *App. Optics.* **42**, 4059 (2003).
18. R. A. Vesey, M. E. Cuneo, G. R. Bennett *et al.*, *Phys. Rev. Lett.* **90**, 035005 (2003).
19. D.L. Hanson, *et.al.* to be submitted for publication.
20. M.E. Cuneo, R.A. Vesey, D.B. Sinars. Accepted for pub, *Phys. Rev. Lett.* (2005)
21. G. B. Zimmerman and W. L. Kruer, *Comm. Plas. Phys. Contr. Fusion* **2**, 51 (1975); J. A. Harte *et al.*, 1996 ICF Annual Report, Lawrence Livermore National Laboratory, Livermore, CA, Report No. UCRL-LR-105821-96, 150 (1997).
22. R.B. Campbell, R. Kodama, T.A. Mehlhorn, K.A. Tanaka, D.R. Welch. *Phys. Rev. Lett.* **94**, p.055001/1-4 (2005)
23. D. R. Welch *et al.*, *Comput. Phys. Commun.* **164**, p183 (2004).
24. R Kodama *et al.*, *Nature* (London) **418**, 933, (2002); also R. Kodama *et al.*, *Plasma Phys. Controlled Fusion* **44**, p109 (2002).
25. R Kodama *et al.*, *Nature* (London) **412**, 798 (2001).
26. H. Alfvén, *Phys. Rev.* **55**, p425 (1939) and M. Honda, *Phys. Plasmas* **7**, 1606 (2000).
27. S. Atzeni. *Phys Plasmas*; **6**, p.3316 (1999)
28. S. A. Slutz, R.A. Vesey. *Phys. Plasmas*, **12**, 062702 (2005).
29. S. A. Slutz and M. C. Herrmann, *Phys. Plasmas* **10**, 234 (2003).